



Iron-catalyzed one-pot sequential transformations: Synthesis of quinazolinones via oxidative Csp³–H bond activation using a new metal-organic framework as catalyst



Tuong A. To^{a,1}, Yen H. Vo^{a,1}, Hue T.T. Nguyen^b, Phuong T.M. Ha^a, Son H. Doan^a, Tan L.H. Doan^b, Shuang Li^c, Ha V. Le^{a,c}, Thach N. Tu^{b,*}, Nam T.S. Phan^{a,*}

^a Faculty of Chemical Engineering, HCMC University of Technology, VNU-HCM, 268 Ly Thuong Kiet, District 10, Ho Chi Minh City, Viet Nam

^b Center for Innovative Materials and Architectures, VNU-HCM, Quarter 6, Linh Trung Ward, Thu Duc District, Ho Chi Minh City, Viet Nam

^c Institute of Chemistry–Functional Materials, Technische Universität Berlin, BA2, Hardenbergstraße 40, 10623 Berlin, Germany

ARTICLE INFO

Article history:

Received 14 April 2018

Revised 20 November 2018

Accepted 23 November 2018

Keywords:

Iron-organic framework

Quinazolinones

Tandem

Csp³–H bond

Catalysis

ABSTRACT

A new mixed-linker iron-based MOF VNU-21 [Fe₃(BTC)(EDB)₂·12.27H₂O] was synthesized via mixed-linker synthetic strategy using 1,3,5-benzenetricarboxylic acid, 4,4'-ethynylendibenzoic acid, and FeCl₂. The VNU-21 was consequently used as a recyclable heterogeneous catalyst in the one-pot synthesis of quinazolinones via two steps under oxygen atmosphere. The synthetic scheme involved iron-catalyzed oxidative Csp³–H bond activation to achieve decarboxylation of phenylacetic acids, and succeeding metal-free oxidative cyclization with 2-aminobenzamides. The VNU-21 was more effective than a series of heterogeneous and homogeneous catalysts. It was possible to reutilize the iron-based framework without a considerable deterioration in catalytic performance. To our best knowledge, this one-pot synthesis of quinazolinones was not previously performed using a recyclable catalyst.

© 2018 Elsevier Inc. All rights reserved.

1. Introduction

Quinazolinones and their derivatives are a well-known class of nitrogen-containing heterocycles, existing in numerous products with significant biological activities [1–3]. A variety of synthetic protocols towards these valuable heterocyclic scaffolds have been explored [4,5]. The synthesis of organic compounds via one-pot multi-step procedures has been considered as an effective and environmentally benign approach, since the isolation of intermediate products is not required, thus minimizing toxic waste and simplifying practical issues [6,7]. López and co-workers previously prepared quinazolinones from 2-nitrobenzamides and aryl aldehydes via a one-pot process [8]. Quinazolinones were also achieved from 2-aminobenzamides and alcohols via one-pot transformations utilizing and FeCl₃ [9], ruthenium complex [10], and iridium complex [11] as catalysts. Hu and co-workers obtained quinazolinones via the same reaction with Fe(NO₃)₃/TEMPO catalyst system [12]. Upadhyaya and co-workers reported a one-pot CuI-catalyzed synthesis of quinazolinones from 2-bromobenzamides and

benzaldehydes, benzyl alcohols, or benzylic hydrocarbons [13]. Yin and co-workers achieved quinazolinones from 2-aminobenzamides and phenylacetic acids via one-pot FeCl₃-catalyzed oxidative functionalization of sp³ C–H bonds, decarboxylation, and subsequent cyclization [14]. To develop greener protocols for the synthesis of quinazolinones, heterogeneous catalysts with advantages of recyclability and reusability should be explored.

The discovery of metal-organic frameworks (MOFs), a new class of crystalline hybrid porous materials, has been considered as one breakthrough in chemistry during the last two decades [15,16]. Integrating interesting properties of both metal nodes and organic linkers, these frameworks have been recognized as potential candidates for a variety of applications, extending from gas capture and storage to catalysis [17–20]. Furthermore, MOFs have been explored to reduce the difference between heterogeneous and homogeneous catalysts owing to their unique features. Among a long series of well-known MOFs, iron-organic frameworks have attracted considerable attention [21–29]. Nevertheless, these MOFs are generally constructed from oxo-centered trimers of octahedral Fe(III) SBUs [21,22,30–32], and indeed, MOFs composed of Fe(II)-based SBUs have been limited in the literature [27,33–35]. In this work, we wish to report the synthesis of a new iron-based MOF, termed VNU-21 (where VNU = Vietnam National University).

* Corresponding authors.

E-mail addresses: tnthach@inomar.edu.vn (T.N. Tu), ptsnam@hcmut.edu.vn (N.T.S. Phan).

¹ These authors contributed equally to this work.

Single crystal analysis revealed that this MOF, formulated as $\text{Fe}_3(\text{BTC})(\text{EDB})_2 \cdot 12.27\text{H}_2\text{O}$ ($\text{BTC}^{3-} = 1,3,5\text{-benzenetricarboxylate}$; $\text{EDB}^{2-} = 4,4'\text{-ethynylenedibenzoate}$), constructed from mixed-linkers of BTC^{3-} , EDB^{2-} and infinite $[\text{Fe}_3(\text{CO}_2)_7]_\infty$ rod SBU. Furthermore, the VNU-21 was utilized as a recyclable catalyst in the one-pot synthesis of quinazolinones, including iron-catalyzed oxidative $\text{Csp}^3\text{-H}$ bond activation to achieve decarboxylation of phenylacetic acids, and succeeding metal-free oxidative cyclization with 2-aminobenzamides.

2. Experimental

2.1. Synthesis of metal-organic framework VNU-21

The mixture of H_2EDB (0.12 g, 0.45 mmol), H_3BTC (0.021 g, 0.1 mmol), and FeCl_2 (0.12 g, 0.94 mmol) was added to DMF (12 mL), and sonicated for 5 min to afford a clear solution. Subsequently, this solution was divided into glass tubes, which were sealed and placed in an isothermal oven, pre-heated at 175 °C, for 72 h, to achieve reddish rhombic prism shape crystals of VNU-21. Consequently, the VNU-21 crystals were exchanged by DMF (5×15 mL), and methanol (5×15 mL). The VNU-21 crystals were then exchanged by liquid CO_2 , evacuated under CO_2 supercritical condition, and activated under dynamic vacuum at room temperature to obtain dried VNU-21 (0.068 g, 75% yield based on H_3BTC). Elemental analysis: $\text{Fe}_3\text{C}_{41}\text{H}_{43.54}\text{O}_{26.27} = \text{Fe}_3(\text{BTC})(\text{EDB})_2 \cdot 12.27\text{H}_2\text{O}$ (Cal: %C = 43.77; %H = 3.87; %N = 0. Found: %C = 43.23; %H = 3.33; %N = 0.26).

2.2. Catalytic studies

In a typical experiment, a solution of phenylacetic acid (0.3 mmol, 40.8 mg) in DMF (0.5 mL) was added to a 10 mL vial with the VNU-21 catalyst (5.5 mg, 5 mol%). The mixture was stirred at 120 °C for 4 h under an oxygen atmosphere. After that, the catalyst was removed by filtration. A solution of 2-aminobenzamide (0.2 mmol, 27.2 mg) in DMSO (0.5 mL) was then added to the reactor. The mixture was additionally stirred at 120 °C for 5 h under oxygen. The GC yield of benzaldehyde and 2-phenylquinazolin-2(3H)-one were monitored by withdrawing samples from the reaction mixture, quenching with brine (1 mL), extracting with ethyl acetate (3×1 mL), drying over anhydrous Na_2SO_4 , and analyzing by GC regarding diphenyl ether as internal standard. After the completion of the second step, the reaction mixture was cooled to room temperature. Resulting solution was quenched with brine (5 mL), extracted by ethyl acetate (3×5 mL), dried over anhydrous Na_2SO_4 prior to the removal of solvent under vacuum. The crude product was purified by silica gel column chromatography using hexane and ethyl acetate (1:1, v/v) as eluent. The structure of 2-phenylquinazolin-4(3H)-one was verified by GC-MS, ^1H NMR and ^{13}C NMR. For the leaching test, after the first 4 h reaction time, the catalyst was removed by filtration. The solution phase was transferred to a new and clean reactor. New phenylacetic acid was added, and the resulting mixture was subsequently stirred for additional 4 h at 120 °C under an oxygen atmosphere. The yield of benzaldehyde was monitored by GC.

3. Results and discussion

3.1. Synthesis and characterization of VNU-21

The iron-based MOF VNU-21 was synthesized in 75% yield via mixed-linker synthetic strategy using 1,3,5-benzenetricarboxylic acid, 4,4'-ethynylenedibenzoic acid, and FeCl_2 . Single crystal X-rays diffraction results indicated that the VNU-21 crystallized in

the orthorhombic space group, *Pbcn* (No. 60), with unit cell parameters, $a = 25.26917$, $b = 33.43879$, and $c = 13.62934$ Å. Indeed, the VNU-21 was identified to possess the same topology with the VNU-20 [36]; however, with the larger pore dimension. Particularly, this material was built from H_3BTC and H_2EDB linkers (Fig. 1a) and the sinusoidal $[\text{Fe}_3(\text{CO}_2)_7]_\infty$ iron-rod SBU [37,38] (Fig. 1b), which was constructed from three distinct octahedral iron centers in consecutive order. The iron centers then connected each other through the sharing edge and vertex to infinite Fe-rod SBU (Fig. 1b). The sinusoidal $[\text{Fe}_3(\text{CO}_2)_7]_\infty$ iron-rod metal cluster was finally joined by the horizontal BTC^{3-} linker (Fig. 1e) and the vertical EDB^{2-} linker (Fig. 1f) to form the 3-dimensional architecture of the VNU-21 (Fig. 1c, d). It should be noted that the VNU-21 possessed open rectangular window of 8.9×12.6 Å² with thick walls architecture, constructed of infinite rings to rings π - π interaction of EDB^{2-} linkers (Fig. 1c, f).

Furthermore, PXRD analysis of the as-synthesized and simulated samples confirmed the bulk phase purity of the obtained VNU-21 (Fig. S1). The VNU-21 was consequently exchanged and activated under CO_2 supercritical condition, for which, the structural maintenance after the activation step was verified by PXRD analysis (Fig. S1). Elemental microanalysis (EA) additionally confirmed the chemical formula of the VNU-21 as $\text{Fe}_3(\text{BTC})(\text{EDB})_2 \cdot 12.27\text{H}_2\text{O}$ (Cal: %C = 43.77; %H = 3.87; %N = 0. Found: %C = 43.23; %H = 3.33; %N = 0.26). Fourier transform-infrared (FT-IR) spectroscopy analysis indicated the existence of the bands centering at 1610 cm^{-1} , which was assigned to $\nu_{\text{C=O}}$ stretch vibration of coordinated carboxylate species in the framework (Fig. S2). The thermal stability of the VNU-21 was investigated by thermogravimetric analysis (TGA). Indeed, TGA result displayed less than 2% weight loss in the range from ambient temperature to 200 °C, and the residual metal oxides, ascribed to Fe_2O_3 , in good agreement with those from model formula (Fig. S3). The permanent porosity of VNU-21 was explored via nitrogen adsorption at 77 K with BET surface areas of $1440\text{ m}^2\text{ g}^{-1}$ being recorded (Fig. S4). Certainly, this number was consistent with the simulated surface areas calculated by utilizing Material Studio 6.0 software ($1419\text{ m}^2\text{ g}^{-1}$). Furthermore, the deconvoluted X-ray photoelectron spectrum (XPS) of the Fe $2p_{3/2}$ region for the VNU-21 showed the peaks attributed to Fe(II) and Fe(III) ions, which are located at 709.5 and 711 eV, respectively (Fig. S5) [35,36]. This result indicated that iron species with the mixed oxidation state are present in the VNU-21 framework.

3.2. Catalytic studies

The VNU-21 was utilized as a heterogeneous catalyst for the one-pot synthesis of 2-phenylquinazolin-4(3H)-one, including iron-catalyzed oxidative $\text{Csp}^3\text{-H}$ bond activation of phenylacetic acid (step 1, Scheme 1), and subsequent oxidative cyclization with 2-aminobenzamide (step 2, Scheme 1). Chen and co-workers previously performed this one-pot transformation to achieve quinazolinones in the presence of FeCl_3 catalyst for 12 h [14]. As the second step proceeded in the absence of the iron-based catalyst, it was decided to separate the VNU-21 after the first step to increase the catalyst lifetime. Preliminary results also indicated that the yield of 2-phenylquinazolin-4(3H)-one was considerably improved if DMSO was utilized as a co-solvent in the second step. Reaction conditions were screened to maximize the yield of the quinazolinone (Table 1). The first step was conducted using 0.22 mmol phenylacetic acid in 0.5 mL solvent 1 at 120 °C for 3 h under an oxygen atmosphere, with 0.01 mmol VNU-21 catalyst. After that, the catalyst was removed, 0.20 mmol 2-aminobenzamide in 0.5 mL solvent 2 was added, and the resulting mixture was heated at 120 °C for 5 h under an oxygen atmosphere. Initially, the impact of solvent in the first step was explored (Entries 1–8, Table 1). It

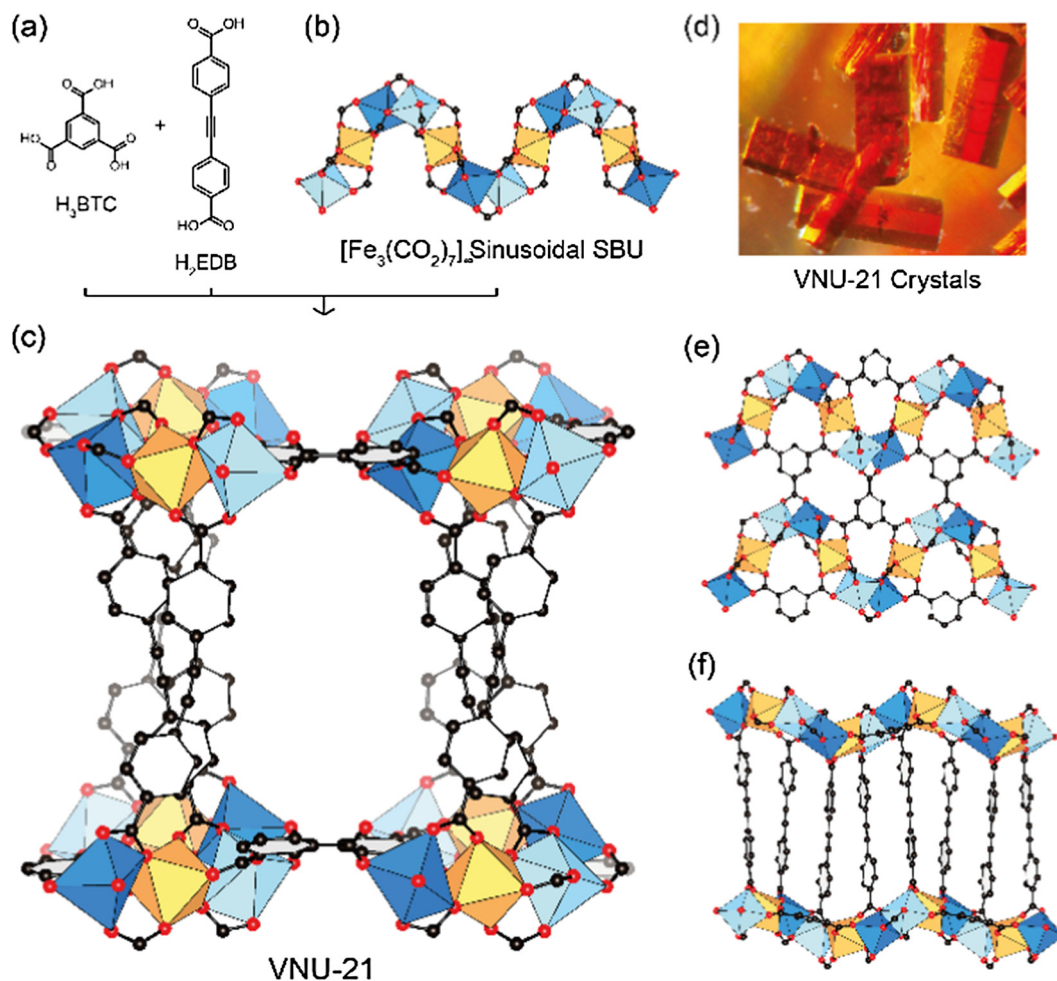
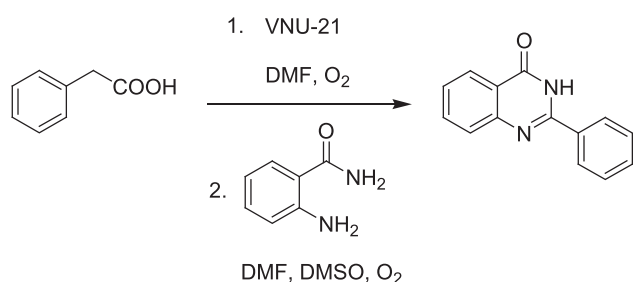


Fig 1. The crystal structure of VNU-21 was assembled from sinusoidal rod $[Fe_3(CO_2)_7]_n$ (b) that are stitched horizontally by BTC^{3-} and vertically by EDB^{2-} (a, e and f) to form the red crystals (d) with structure highlighted by a rectangular window of $8.9 \times 12.6 \text{ \AA}^2$ (c). Atom colors: Fe, blue, light blue and orange polyhedra; C, black; O, red. All H atoms are omitted for clarity. (For interpretation of the references to colour in this figure legend, the reader is referred to the web version of this article.)



Scheme 1. Synthesis of 2-phenylquinazolin-4(3H)-one via one-pot two-step.

was observed that the first step of the transformation was favored in DMF as solvent, affording 2-phenylquinazolin-4(3H)-one in 36% yield (Entry 1, Table 1). DMA exhibited similar performance with 31% yield being detected, while NMP, chlorobenzene, dichlorobenzene, *p*-xylene, diglyme, and diethyl carbonate should not be used (Entries 2–8, Table 1).

Having these results, we consequently investigated the impact of phenyl acetic acid: 2-aminobenzamide molar ratio on the yield of 2-phenylquinazolin-4(3H)-one (Entries 9–13, Table 1). Experimental results indicated that the reaction was favored by excess amounts of phenylacetic acid. The reaction afforded 34% yield when 1 equivalent of phenylacetic acid was used (Entry 9, Table 1).

Increasing the amount of phenylacetic acid to 1.5 equivalents, the yield of 2-phenylquinazolin-4(3H)-one was improved to 67% (Entry 12, Table 1). One more factor that must be explored is the amount of the VNU-21 catalyst (Entries 15–18, Table 1). Noted that only 3% yield was recorded in the absence of the catalyst, thus verifying the requirement of the iron-organic framework for the transformation (Entry 15, Table 1). The yield was considerably improved in the presence of the framework catalyst, affording 67% for the reaction utilizing 3.3 mol% catalyst (Entry 16, Table 1). It was noticed that by increasing the reaction of the first step to 4 h, the yield of 2-phenylquinazolin-4(3H)-one was remarkably upgraded to 89% in the presence of 3.3 mol% catalyst (Entry 19, Table 1). The influence of solvent in the second step on the yield of 2-phenylquinazolin-4(3H)-one was also studied (Entries 19–25, Table 1). It was noted that DMSO was the solvent of choice for the second step (Entry 19, Table 1). Other solvents, including DMF, chlorobenzene, dichloroethane, diethyl carbonate, dioxane, and *tert*-butanol exhibited low performance for the transformation (Entries 20–25, Table 1).

Since the one-pot synthesis of 2-phenylquinazolin-4(3H)-one from phenylacetic acid and 2-aminobenzamide utilizing the VNU-21 catalyst was conducted in liquid phase, an essential aspect that should be studied is the leaching of iron species from the framework to the solution. Control experiments were consequently performed to verify if the transformation proceeded via truly heterogeneous catalysis or not. Noted that the first step

Table 1
Screening reaction conditions to maximize yield of 2-phenylquinazolin-4(3H)-one.^a

Entry	Solvent 1 (0.5 mL)	Reactant 1 (mmol)	Catalyst (mmol)	Temperature (°C)	Reactant 2 (mmol)	Solvent 2 (0.5 mL)	Yield (%)
1	DMF	0.22	0.01	120	0.20	DMSO	36
2	DMA	0.22	0.01	120	0.20	DMSO	31
3	NMP	0.22	0.01	120	0.20	DMSO	3
4	Chlorobenzene	0.22	0.01	120	0.20	DMSO	18
5	DCB	0.22	0.01	120	0.20	DMSO	12
6	p-xylene	0.22	0.01	120	0.20	DMSO	5
7	Diglyme	0.22	0.01	120	0.20	DMSO	8
8	DEC	0.22	0.01	120	0.20	DMSO	5
9	DMF	0.20	0.01	120	0.20	DMSO	34
10	DMF	0.22	0.01	120	0.20	DMSO	36
11	DMF	0.25	0.01	120	0.20	DMSO	40
12	DMF	0.30	0.01	120	0.20	DMSO	67
13	DMF	0.60	0.01	120	0.20	DMSO	70
14	DMF	0.30	0	120	0.20	DMSO	3
15	DMF	0.30	0.005	120	0.20	DMSO	42
16	DMF	0.30	0.01	120	0.20	DMSO	67
17	DMF	0.30	0.015	120	0.20	DMSO	69
18	DMF	0.30	0.02	120	0.20	DMSO	72
19	DMF	0.30	0.01	120	0.20	DMSO	89 ^b
20	DMF	0.30	0.01	120	0.20	DMF	16 ^b
21	DMF	0.30	0.01	120	0.20	chlorobenzene	41 ^b
22	DMF	0.30	0.01	120	0.20	DCE	5 ^b
23	DMF	0.30	0.01	120	0.20	DEC	25 ^b
24	DMF	0.30	0.01	120	0.20	dioxane	8 ^b
25	DMF	0.30	0.01	120	0.20	tert-butanol	14 ^b

^a The first step was conducted for 3 h under an oxygen atmosphere; the second step was conducted for 5 h under an oxygen atmosphere; DMF: N,N'-dimethylformamide; DMA: Dimethylacetamide; DMSO: Dimethyl sulfoxide; NMP: N-Methyl-2-pyrrolidone; DCB: dichlorobenzene; DEC: diethyl carbonate; DCE: dichloroethane.

^b The first step was conducted for 4 h under an oxygen atmosphere. GC yield of 2-phenylquinazolin-4(3H)-one.

involved iron-catalyzed oxidative Csp³–H bond activation of phenylacetic acid to produce benzaldehyde (step 1, Scheme 1), while the oxidative cyclization of benzaldehyde with 2-aminobenzamide (step 2, Scheme 1) proceeded under metal-free conditions. We consequently explored the contribution of soluble iron species, if any, to the formation of benzaldehyde in the first step. The first step was conducted using 0.3 mmol phenylacetic acid in 0.5 mL DMF at 120 °C for 4 h under an oxygen atmosphere, with 0.01 mmol VNU-21 catalyst. After the experiment, the VNU-21 catalyst was separated from the mixture. The liquid phase was transferred to a second reactor, and fresh phenylacetic acid was subsequently added to the reactor. The resulting mixture was heated at 120 °C for 4 h under an oxygen atmosphere. Yield of benzaldehyde was monitored by GC. It was noticed that almost no additional benzaldehyde was generated under these conditions (Leaching test 1, Fig. 2). In a second experiment, after the first 90 min reaction time with 40% yield of benzaldehyde being

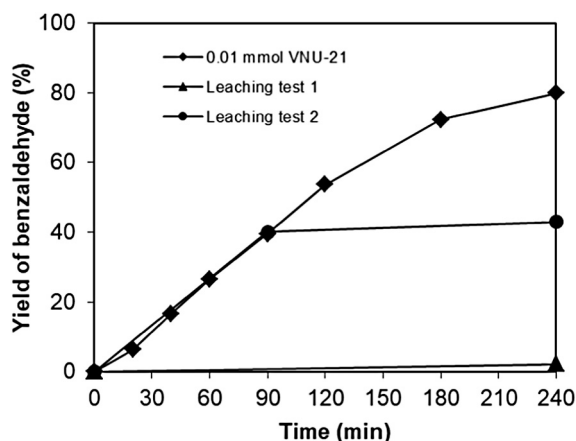


Fig. 2. Leaching test showed that the first step did not proceed in the absence of the VNU-21.

detected, the VNU-21 catalyst was isolated by centrifugation. The DMF solution was transferred to a second reactor, and the mixture was heated at 120 °C for further 150 min. Similar to the first leaching experiment, no additional benzaldehyde was recorded after the catalyst removal (Leaching test 2, Fig. 2). Moreover, ICP analyses of the fresh and spent catalysts were carried out, indicating that the amount of iron in the VNU-21 remained unchanged during the experiment (16% wt/wt). Additionally, ICP analysis of the filtrate showed that less than 1% of iron (compared to the total amount of iron in the catalyst) was soluble in the solution. These data would verify that the oxidative Csp³–H bond activation of phenylacetic acid to produce benzaldehyde (step 1, Scheme 1) only proceeded in the presence of the solid VNU-21 catalyst.

To emphasize the positive aspects of utilizing the VNU-21 as catalyst for the one-pot synthesis of 2-phenylquinazolin-4(3H)-one from phenylacetic acid and 2-aminobenzamide, a series of heterogeneous and homogeneous catalysts were also tested for this transformation. The first step was conducted using 0.22 mmol phenylacetic acid in 0.5 mL DMF at 120 °C for 4 h under an oxygen atmosphere, with 0.01 mmol catalyst. After that, the solid catalyst was removed, 0.20 mmol 2-aminobenzamide in 0.5 mL DMSO was added, and the resulting mixture was heated at 120 °C for 5 h under an oxygen atmosphere. The reaction using FeCl₃ proceeded to 67% yield of 2-phenylquinazolin-4(3H)-one, while 33% yield was obtained for the case of FeSO₄. This observation suggested that both Fe(II) and Fe(III) species were active for the transformation. Indeed, it was previously reported that both Fe(II) and Fe(III) catalysts could be used for similar transformations [14,39–41]. Fe₃O(BDC)₃ [BDC = 1,4-benzenedicarboxylate] was more active towards the reaction, affording 72% yield. Fe₃O(BPDC)₃ [BPDC = 4,4'-biphenyldicarboxylate] was noticed to exhibit higher activity, with 85% yield of 2-phenylquinazolin-4(3H)-one being achieved. MOFs containing other metals were less active than Fe-MOFs in the oxidative Csp³–H bond activation of phenylacetic acid, producing the desired quinazolinone product in lower yields. The reaction using Cu₂(OBA)₂(BPY) [OBA = 4,4'-oxybis(benzoate); BPY = 4,4'-bipyridine] catalyst afforded 46% yield, while only 12% yield was

noticed for that utilizing Cu-MOF-199 as catalyst. Zr-MOF-808 was almost inactive for the reaction, affording only 3% yield. Similarly, the reaction utilizing Co-ZIF-67 catalyst progressed with difficulty, with only 2% yield being detected. It should be noted that FeBTC [BTC = 1,3,5-benzenetricarboxylate], the Fe-MOF prepared using 1,3,5-benzenetricarboxylic acid linker, exhibited low activity for

the transformation, affording only 10% yield. The low catalytic activity of the FeBTC can be attributed to the low activity of the iron trimesic cluster comparing with the rod-based iron cluster in the VNU-21. Additionally, VNU-20, the mixed linker Fe-MOF synthesized from 1,3,5-benzenetricarboxylic acid and 2,6-naphthalenedicarboxylic acid, was used. The VNU-21 possessed the same topology with the VNU-20 [36], however with the larger pore dimension ($8.9 \times 12.6 \text{ \AA}^2$ vs $6.0 \times 8.7 \text{ \AA}^2$). Under these conditions, the VNU-20 was less active than the VNU-21, offering 78% yield. Compared to these catalysts, the VNU-21 displayed the best performance, with 89% yield being achieved (Fig. 3).

To gain insight into the reaction pathway, several control experiments were carried out (Scheme 2). First, the yield of benzaldehyde (**2**) in the first step was significantly decreased in the presence of (2,2,6,6-tetramethylpiperidin-1-yl)oxy (TEMPO) as a radical scavenger (Scheme 2a). This result verified that the oxidative decarboxylation of phenylacetic acid (**1**) progressed via a radical pathway. In the next two experiments, we tried to determine intermediates of this process (Scheme 2b and 2c). High yields of **2** were obtained when mandelic acid (**A**) and benzoylformic acid (**B**) (in the absence of VNU-21) were employed as reactant in the first step of our protocol, suggesting that these two acids could be the intermediates. The second step pathway was also investigated by the next two experiments (Scheme 2d and e). 2-Phenylquinazolin-4(3H)-one (**4**) was produced in excellent yield when 2-aminobenzamide (**3**) and benzaldehyde (**2**) was employed (Scheme 2d), while the yield declined to 59% when molecular sieve was added (Scheme 2e). Therefore, water could play a vital role on this step. On the basis of these results and previous reports in the literature [14,42], a plausible mechanism was proposed (Scheme 3).

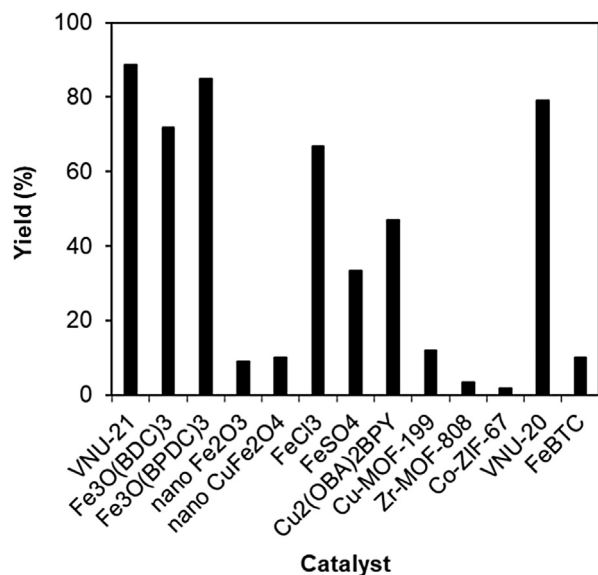
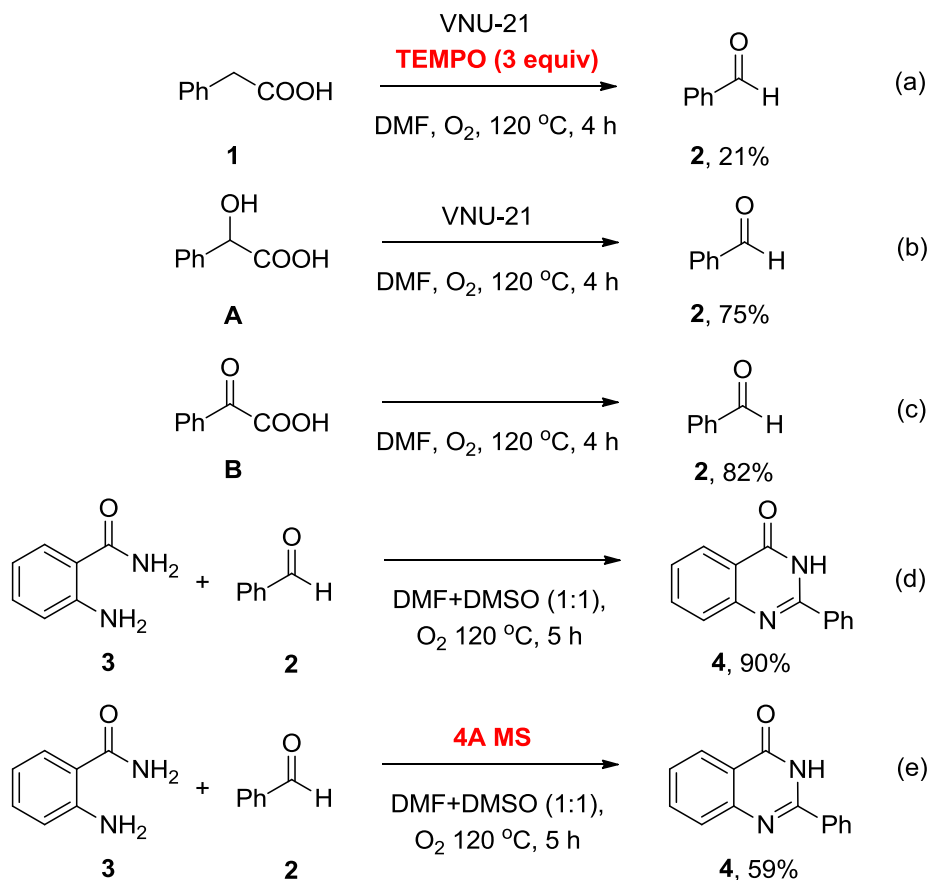
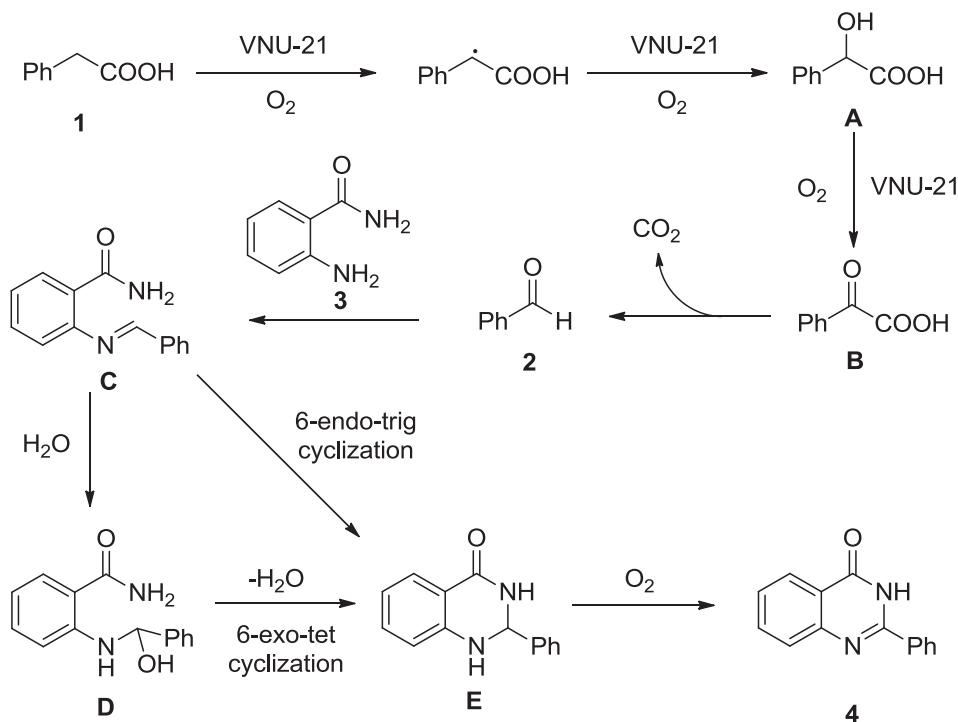


Fig. 3. Yield of 2-phenylquinazolin-4(3H)-one vs different catalysts.



Scheme 2. Control experiments.



Scheme 3. Proposed reaction pathway.

Under VNU-21 catalysis, α -hydroxycarboxylic acid **A** was formed by aerobic oxidation via radical pathway following by dehydrogenation to afford α -ketoacid **B**. Aromatic aldehyde **2** was then produced by decarboxylation of **B** [14]. After the first step, **3** was added to the reaction and reacted with **2** to obtain imine **C**. Intermediate **E** was generated by a 6-*endo*-trig cyclization of **C**. The presence of water in the reaction media could accelerate the cyclization through intermediate **D** which was produced by nucleophilic addition of water to **C**. 6-*Exo*-tet cyclization of **D** subsequently occurred, creating intermediate **E**. Finally, product **4** was formed by oxidative dehydrogenation of **E** in the presence of oxygen (Scheme 3) [42]. From experimental point of view, it should be noted that performing the catalyst-free cyclization of benzaldehyde with 2-aminobenzamide resulted in a large amount of benzoic acid as a by-product, while no trace amount of benzoic acid was detected for the transformation starting with phenylacetic acid. Apparently, benzaldehyde was readily oxidized to benzoic acid under these reaction conditions. Indeed, Yin and co-workers previously utilized phenylacetic acids instead of benzaldehydes in a one-pot synthesis of quinazolinone [14]. Song and co-workers employed phenylacetic acids instead of benzaldehydes in the synthesis of 2-aryl benzothiazoles and benzonitriles [43,44]. Chaskar and co-workers demonstrated an efficient synthesis of benzoic acids from phenylacetic acids instead of benzaldehydes [45].

As previously mentioned, the VNU-21 exhibited higher catalytic performance than a variety of homogeneous and heterogeneous catalysts. To additionally highlight the environmentally benign aspect of this iron-based framework, the readiness of catalyst recovery and reutilization was consequently studied. The first step was carried out using 0.3 mmol phenylacetic acid in 0.5 mL DMF at 120 °C for 4 h under an oxygen atmosphere, with 0.01 mmol catalyst. After that, the solid VNU-21 catalyst was removed by centrifugation, 0.20 mmol 2-aminobenzamide in 0.5 mL DMSO was added,

and the resulting mixture was heated at 120 °C for 5 h under an oxygen atmosphere. The recovered framework was then washed thoroughly with DMF, and methanol to get rid of any physisorbed materials, and consequently activated under vacuum at ambient temperature on a Shlenk line for 1 h. New catalytic experiment was thereafter carried out using the recovered catalyst under the same conditions. Experimental data indicated that it was possible to reuse the VNU-21 catalyst for the one-pot synthesis of 2-phenylquinazolin-4(3H)-one from phenylacetic acid and 2-aminobenzamide without a noticeable deterioration in catalytic efficiency. Certainly, 88% yield of 2-phenylquinazolin-4(3H)-one was obtained in the 5th run (Fig. 4). The FT-IR analysis results of both fresh reutilized VNU-21 samples displayed similar absorption characteristics (Fig. 5). Additionally, the XRD result of the reutilized catalyst suggested that the iron-based framework maintained

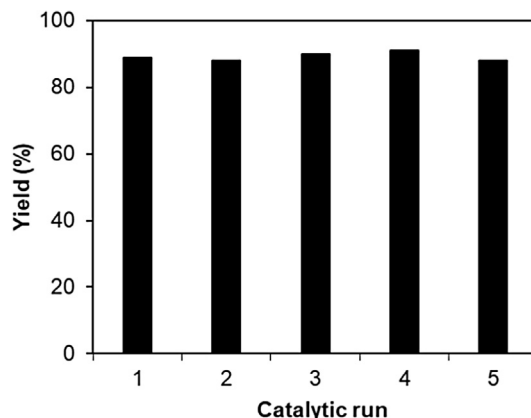


Fig. 4. Catalyst reutilization studies.

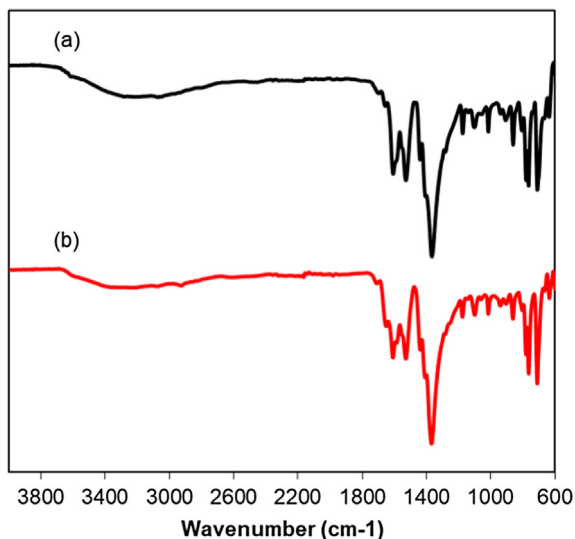


Fig. 5. FT-IR spectra of the fresh (a) and recovered (b) VNU-21 catalyst.

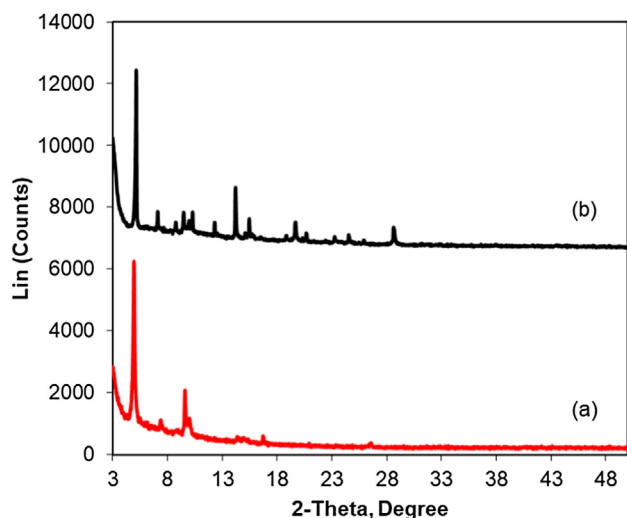


Fig. 6. X-ray powder diffractograms of the fresh (a) and recovered (b) VNU-21 catalyst.

its crystallinity, though a slight difference was recorded (Fig. 6). No significant changes were observed in the Fe 2p XPS spectra of the material before and after the catalysis. Importantly, the ratio of Fe(II)/Fe(III) in the VNU-21 was found to be unchanged, i.e. approximately 46% based on the area of the deconvoluted Fe 2p_{3/2} feature peaks, further indicating that the VNU-21 framework containing mixed-valence iron species was stable under the applied reaction conditions (Fig. 7).

The scope of this work was subsequently extended to the synthesis of different quinazolinones via oxidative Csp³–H bond activation using the VNU-21 catalyst (Table 2). The first step was conducted using 0.3 mmol phenylacetic acid in 0.5 mL DMF at 120 °C for 4 h under an oxygen atmosphere, with 0.01 mmol catalyst. After that, the solid catalyst was removed, 0.20 mmol 2-aminobenzamide in 0.5 mL DMSO was added, and the resulting mixture was heated at 120 °C for 5 h under an oxygen atmosphere. Following this procedure, 2-phenylquinazolin-4(3H)-one was achieved in 87% isolated yield (Entry 1). Phenylacetic acids containing an electron-withdrawing substituent was noticed to be less reactive, and the reaction time of the second step had to be extended to 12 h (Entries 2–4). Moving to 2-chlorophenylacetic acid, 93% yield of 2-(2-chlorophenyl)quinazolin-4(3H)-one was obtained, though the reaction time of the second step had to be extended to 18 h (Entry 5). Phenylacetic acids containing an electron-donating substituent was more reactive, affording 2-(4-methoxyphenyl)quinazolin-4(3H)-one (Entry 6) and 2-(3-methoxyphenyl)quinazolin-4(3H)-one (Entry 7) in 97% and 96% yields, respectively. However, 2-*o*-tolylquinazolin-4(3H)-one was obtained in 74% yield for the case of 2-methylphenylacetic acid (Entry 8). 2-(thiophen-3-yl)acetic acid was also reactive, producing 2-(thiophen-3-yl)quinazolin-4(3H)-one (Entry 9) in 79% yields. Moving to 2-aminobenzamides containing a substituent, corresponding quinazolinones were also achieved in high yields (Entries 10–12). The research scope was additionally expanded to the synthesis of phenyl benzimidazoles in the presence of the VNU-21 catalyst. Under these conditions, 2-phenyl-1H-benzo[d]imidazole (Entry 13) was produced in 87% yield from phenylacetic acid and *o*-phenylenediamine. Similarly, other phenyl benzimidazoles were achieved in high yields from substituted *o*-phenylenediamines (Entries 14–16). 2-Aminobenzenethiol, and 2-aminophenol were less reactive towards the one-pot transformation, with 2-phenylbenzo[d]thiazole (Entry 17), and 2-phenylbenzo[d]oxazole (Entry 18) being obtained in 60% and 10% yields, respectively.

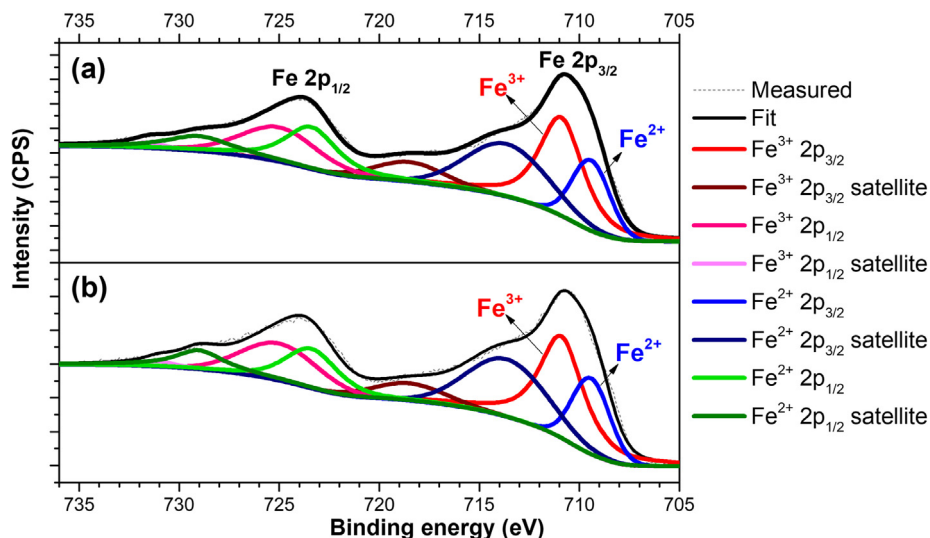


Fig. 7. Fe 2p XPS spectra of the fresh (a) and recovered (b) VNU-21 catalyst.

Table 2
 Synthesis of different quinazolinones via oxidative Csp³–H bond activation using VNU-21 catalyst.^a

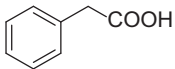
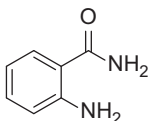
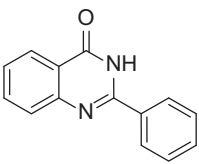
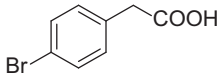
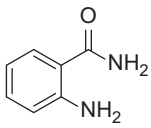
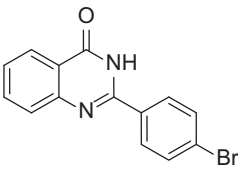
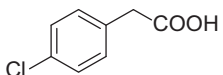
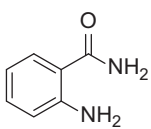
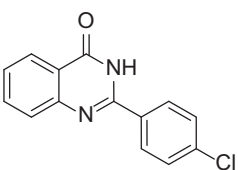
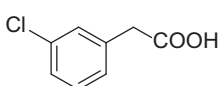
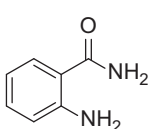
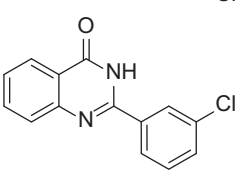
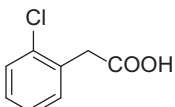
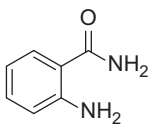
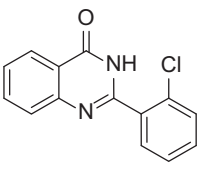
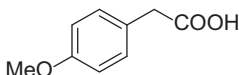
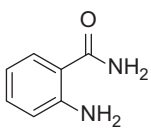
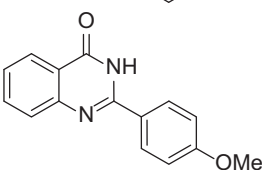
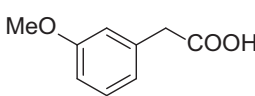
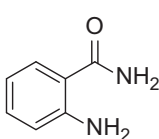
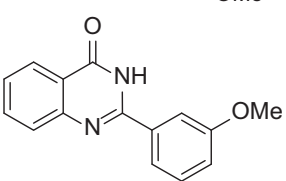
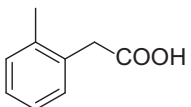
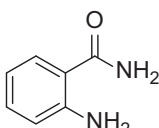
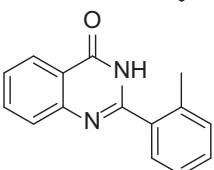
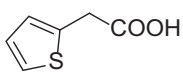
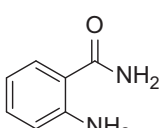
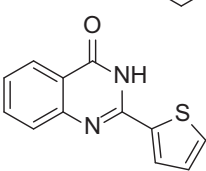
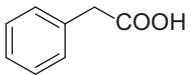
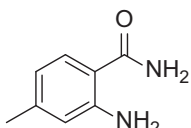
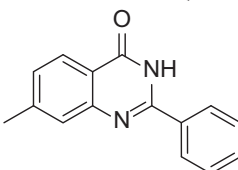
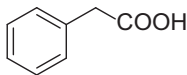
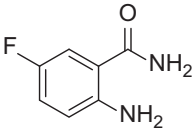
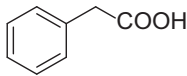
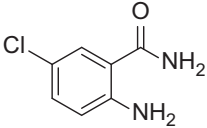
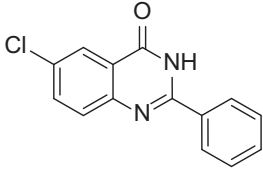
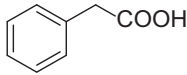
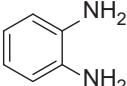
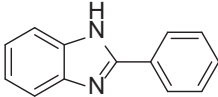
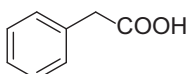
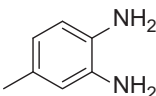
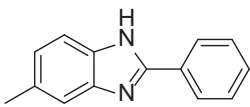
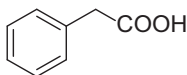
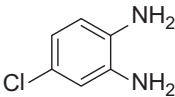
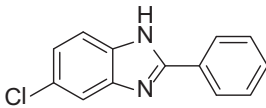
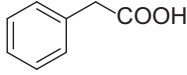
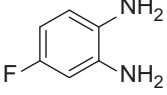
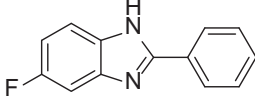
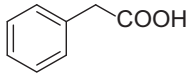
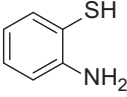
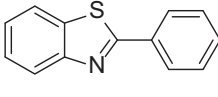
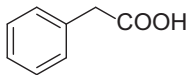
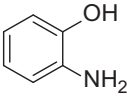
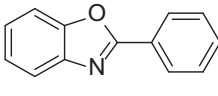
Entry	Reactant 1	Reactant 2	Product	Yield ^b
1				87
2				73 ^c
3				78 ^c
4				86 ^c
5				93 ^d
6				97
7				96
8				74 ^c
9				79 ^d
10				90

Table 2 (continued)

Entry	Reactant 1	Reactant 2	Product	Yield ^b
11				87
12				90
13				87
14				93
15				98
16				76
17				60
18				10

^a First step: phenylacetic acid (0.3 mmol), DMF (0.5 mL), VNU-21 (0.01 mmol), 120 °C, 4 h, oxygen atmosphere; second step: 2-aminobenzamides/o-substituted anilines (0.2 mmol), DMSO (0.5 mL), 5 h, oxygen atmosphere.

^b Isolated yield.

^c Second step: 12 h.

^d Second step: 18 h.

4. Conclusions

A new iron-based MOF, VNU-21 ($\text{Fe}_3(\text{BTC})(\text{EDB})_2 \cdot 12.27\text{H}_2\text{O}$), constructed from mixed-linkers of BTC^{3-} and EDB^{2-} with infinite $[\text{Fe}_3(\text{CO}_2)_7]_\infty$ rod SBU, was synthesized and characterized by several techniques. The VNU-21 was consequently used as a recyclable heterogeneous catalyst in the one-pot synthesis of quinazolinones via two steps under oxygen atmosphere. The first step involved the decarboxylation of phenylacetic acids via iron-catalyzed oxidative Csp³–H bond activation. The second step was the metal-free oxidative cyclization of intermediate products with 2-aminobenzamides to produce corresponding quinazolinones. The transformation was remarkably regulated by the solvent, in which DMF should be used for the first step, while DMSO emerged as the solvent of choice for the second step. The VNU-21 was more active towards the one-pot synthesis of quinazolinones than a series of heterogeneous and homogeneous catalysts. It was possible to reuse the iron-based framework without a considerable deterioration in catalytic performance. The point that quinazolinones were generated via one-pot sequential transformations with a

recyclable catalyst was consequently valuable to organic synthesis and the chemical industry.

Acknowledgements

Thach N. Tu acknowledges the Naval International Cooperative Opportunities in Science and Technology Program through Project No. N62909-16-1-2146 for VNU-21 synthesis and characterization. The catalytic studies were financially supported by the Viet Nam National Foundation for Science and Technology Development (NAFOSTED) under Project code 104.05-2017.32.

Appendix A. Supplementary material

Supplementary data to this article can be found online at <https://doi.org/10.1016/j.jcat.2018.11.031>.

References

- [1] T. Abe, Y. Takahashi, Y. Matsubara, K. Yamada, *Org. Chem. Front.* 4 (2017) 2124–2127.

- [2] A.V.A. Gholap, S. Maity, C. Schulzke, D. Maiti, A.R. Kapdi, *Org. Biomol. Chem.* 15 (2017) 7140–7146.
- [3] D.N. Garad, S.B. Mhaske, *J. Org. Chem.* 82 (2017) 10470–10478.
- [4] T.M.M. Maiden, J.P.A. Harrity, *Org. Biomol. Chem.* 14 (2016) 8014–8025.
- [5] B.-Q. Hu, J. Cui, L.-X. Wang, Y.-L. Tang, L. Yang, *RSC Adv.* 6 (2016) 43950–43953.
- [6] Y. Hayashi, *Chem. Sci.* 7 (2016) 866–880.
- [7] G. Szöllösi, *Catal. Sci. Technol.* (2018), <https://doi.org/10.1039/C7CY01671A>, in press.
- [8] A.H. Romero, J. Salazar, S.E. López, *Synthesis* 45 (2013) 2043–2050.
- [9] D. Zhao, Y.-R. Zhou, Q. Shen, J.-X. Li, *RSC Adv.* 4 (2014) 6486–6489.
- [10] A.J.A. Watson, A.C. Maxwell, J.M. Williams, *Org. Biomol. Chem.* 10 (2012) 240–243.
- [11] J. Zhou, J. Fang, *J. Org. Chem.* 76 (2011) 7730–7736.
- [12] Y. Hu, L. Chen, B. Li, *RSC Adv.* 6 (2016) 65196–65204.
- [13] K. Upadhyaya, R.K. Thakur, S.K. Shukla, R.P. Tripathi, *J. Org. Chem.* 81 (2016) 5046–5055.
- [14] X. Chen, T. Chen, F. Ji, Y. Zhou, S.-F. Yin, *Catal. Sci. Technol.* 5 (2015) 2197–2202.
- [15] G. Maurin, C. Serre, A. Cooper, G. Férey, *Chem. Soc. Rev.* 46 (2017) 3104–3107.
- [16] W. Xu, K.B. Thapa, Q. Ju, Z. Fang, W. Huang, *Coord. Chem. Rev.* 373 (2018) 199–232.
- [17] K. Adil, Y. Belmabkhout, R.S. Pillai, A. Cadiou, P.M. Bhatt, A.H. Assen, G. Maurin, M. Eddaoudi, *Chem. Soc. Rev.* 46 (2017) 3402–3430.
- [18] S.M.J. Rogge, A. Bavykina, J. Hajek, H. Garcia, A.I. Olivos-Suarez, A. Sepúlveda-Escribano, A. Vimont, G. Clet, P. Bazin, F. Kapteijn, M. Daturi, E.V. Ramos-Fernandez, F.X.L.i. Xamena, V.V. Speybroeck, J. Gascon, *Chem. Soc. Rev.* 46 (2017) 3134–3184.
- [19] Y. Wen, J. Zhang, Q. Xu, X.-T. Wu, Q.-L. Zhu, *Coord. Chem. Rev.* 376 (2018) 248–276.
- [20] R. Yu-Zhen Chen, L. Zhang, H.-L. Jiang Jiao, *Coord. Chem. Rev.* 362 (2018) 1–23.
- [21] K. Wang, D. Feng, T.F. Liu, J. Su, S. Yuan, Y.P. Chen, M. Bosch, X. Zou, H.C. Zhou, *J. Am. Chem. Soc.* 136 (2014) 13983–13986.
- [22] D. Lv, H. Wang, Y. Chen, F. Xu, R. Shi, Z. Liu, X. Wang, S.J. Teat, Q. Xia, Z. Li, J. Li, *ACS Appl Mater. Interfaces* 10 (2018) 6031–6038.
- [23] L. Hanna, P. Kucheryavy, C. Liu, X. Zhang, J.V. Lockard, *J. Phys. Chem. C* 121 (2017) 13570–13576.
- [24] S. Hou, Y.-N. Wu, L. Feng, W. Chen, Y. Wang, C. Morlay, F. Li, *Dalton Trans.* 47 (2018) 2222–2231.
- [25] Y. Han, Y. Zhang, Y. Zhang, A. Cheng, Y. Hu, Z. Wang, *Appl. Catal. A. Gen.* 564 (2018) 183–189.
- [26] C. Gao, S. Chen, X. Quan, H. Yu, Y. Zhang, *J. Catal.* 356 (2017) 125–132.
- [27] J. Tang, J. Wang, *Environ. Sci. Technol.* 52 (2018) 5367–5377.
- [28] A. Dhakshinamoorthy, M. Alvaro, H. Garcia, *J. Catal.* 289 (2012) 259–265.
- [29] A. Ramirez, L. Gevers, A. Bavykina, S. Ould-Chikh, J. Gascon, *ACS Catal.* 8 (2018) 9174–9182.
- [30] H. Chevreau, A. Permyakova, F. Nouar, P. Fabry, C. Livage, F. Ragon, A. Garcia-Marquez, T. Devic, N. Steunou, C. Serre, P. Horcajada, *CrystEngComm* 18 (2016) 4094–4101.
- [31] D. Wang, S.E. Gilliland III, X. Yi, K. Logan, D.R. Heitger, H.R. Lucas, W.-N. Wang, *Environ. Sci. Technol.* 52 (2018) 4275–4284.
- [32] Y. Georgiou, J.A. Perman, A.B. Bourlinos, Y. Deligiannakis, *J. Phys. Chem. C* 122 (2018) 4859–4869.
- [33] K. Kongpatpanich, S. Horike, M. Sugimoto, S. Kitao, M. Seto, S. Kitagawa, *Chem. Commun.* 50 (2014) 2292–2294.
- [34] D.J. Xiao, E.D. Bloch, J.A. Mason, W.L. Queen, M.R. Hudson, N. Planas, J. Borycz, A.L. Dzubak, P. Verma, K. Lee, F. Bonino, V. Crocella, J. Yano, S. Bordiga, D.G. Truhlar, L. Gagliardi, C.M. Brown, J.R. Long, *Nat. Chem.* 6 (2014) 590–595.
- [35] M. Pu, Y. Ma, J. Wan, Y. Wang, J. Wang, M.L. Brusseau, *Catal. Sci. Technol.* 7 (2017) 1129–1140.
- [36] P.H. Pham, S.H. Doan, H.T.T. Tran, N.N. Nguyen, A.N.Q. Phan, H.V. Le, T.N. Tu, N. T.S. Phan, *Catal. Sci. Technol.* 8 (2018) 1267–1271.
- [37] T.-Z. Zhang, Y. Lu, Y.-G. Li, Z. Zhang, W.-L. Chen, H. Fu, E.-B. Wang, *Inorganica Chim. Acta* 384 (2012) 219–224.
- [38] Y.-W. Li, J.-P. Zhao, L.-F. Wang, X.-H. Bu, *CrystEngComm* 13 (2011) 6002–6006.
- [39] J.D. Houwer, K.A. Tehrani, B.U.W. Maes, *Angew. Chem. Int. Ed.* 124 (2012) 2799–2802.
- [40] M. Nakanishi, C. Bolm, *Adv. Synth. Catal.* 349 (2007) 861–864.
- [41] B. Join, K. Mçller, C. Ziebart, K. Schrçder, D. Gçrdes, K. Thurow, A. Spannenberg, K. Junge, M. Beller, *Adv. Synth. Catal.* 353 (2011) 3023–3030.
- [42] N.Y. Kim, C.-H. Cheon, *Tetrahedron Lett.* 55 (2014) 2340–2344.
- [43] Q. Song, Q. Feng, M. Zhou, *Org. Lett.* 15 (2013) 5990–5993.
- [44] Q. Feng, Q. Song, *Adv. Synth. Catal.* 356 (2014) 1697–1702.
- [45] H.P. Kalmode, K.S. Vadagaonkar, S.L. Shinde, A.C. Chaskar, *J. Org. Chem.* 82 (2017) 3781–3786.